Comparative Study of Numerical Modelling Techniques to Estimate Tidal Turbine Blade Loads

Kate Porter[#1], Stephanie Ordonez-Sanchez[#2], Thomas Nevalainen[#3], Song Fu[#4], Cameron Johnstone[#5]

[#]*Department of Mechanical and Aerospace Engineering, University of Strathclyde*
Montrose Street, Glasgow, G1 1XJ, UK

[1]kate.porter@strath.ac.uk

[2]s.ordonez@strath.ac.uk

[3]thomas.nevalainen@strath.ac.uk

[4]song.fu@strath.ac.uk

[5]cameron.johnstone@strath.ac.uk

***Abstract*— This paper presents a method to obtain the pressure distribution across the surface of a tidal turbine blade, but without the extensive computational time that is required by 3D CFD modelling. The approach uses a combination of blade element momentum theory (BEMT) and 2D CFD modelling, where the inflow velocity vector for each blade element computed from the BEMT model is input to a 2D CFD model of each of the blade sections. To assess the validity of this approach, a comparison is made with both a BEMT and a 3D CFD model for three different blade profiles at full scale (NACA 63-8xx, NREL S814 and Wortmann FX 63-137). A comparison is also made of the NREL blade at smaller scale to investigate any Reynolds number effects on the model performance. The agreement is shown to be very reasonable between the three methods, although the forces are consistently slightly over-predicted by the BEMT method compared to the 2D-CFD-BEMT model, and the 2D-CFD-BEMT model over-predicts the pressure along the leading edge compared to the 3D CFD results. The proposed method is shown to be particularly useful when conducting initial blade structural analysis under dynamic loading.**

***Keywords*— Blade element momentum theory; blade loading; CFD; model comparison; tidal turbine**

I. INTRODUCTION

Tidal energy is developing rapidly and is on the brink of becoming a viable alternative to traditional carbon intensive energy generation methods, with the first near-commercial tidal farm currently being installed off the Orkney coast [1]. However, there are several key areas in which further research is warranted to help to realise this technology. One of these is illustrated by a number of blade failures during recent field tests of prototype turbines [2] which can be attributed to a lack of knowledge of the complex hydrodynamic loading patterns seen by the turbines in the marine environment. It is clear that there is a need to better understand the effects of dynamic loading on blade structural and fatigue performance. This will enable the selection of the most suitable materials and optimisation of the blade structural design thereby improving blade reliability, survivability and reducing costs, all of which are key to establishing the financial viability of the industry.

Turbine blade loading can be investigated by conducting physical tests in the field or at smaller scale in the laboratory, or through the use of computational modelling.

Experimental and field studies do not require any assumptions to be made about the interactions between the flow and turbine structure, and they are also very useful for understanding practical issues of operation and performance. However, these types of tests are expensive and, therefore, usually time limited. Consequently they do not allow a wide range of options to be tested, rather a single prototype design is studied. Furthermore, limitations in the measurement systems mean that the pressure distribution over the blade surface is not fully captured. Instead the force measurements are often confined to the turbine shaft [3] or to the blade root sections [4]. Tests run in the laboratory at small scale are not in similitude with larger scale studies, which introduces some uncertainty when these tests are used to predict turbine behaviour at the full scale.

Analytical or numerical modelling offers a much less expensive approach that enables all variables to be changed readily, providing a very useful tool for initial modelling and optimisation studies regarding blade structural design and power capture performance. These models can also be used to provide a link between experiments conducted at different scales. However, computational approaches contain a number of simplifications compared to real flows and are limited by the assumptions inherent in the models. Therefore, comparison with experimental and/or field test results is advisable, and a tandem approach is recommended where computational modelling is supported by a limited number of laboratory/field tests during progression through the technology readiness levels (TRLs) [5].

In terms of computational modelling there are a variety of approaches available for estimating the forces on tidal turbine blades, including blade element momentum theory (BEMT), lifting line theory and computational fluid dynamics (CFD). These differ in terms of accuracy, computational time and the outputs that are computed.

The simplest approach is BEMT. The blade is split into a number of elements along the blade radius and a pair of point loads (normal and tangential to the plane of rotation) are

generated at the centre of each of these. In contrast, CFD is the most complex approach which numerically solves the Navier-Stokes equations at a mesh of points over the entire blade surface. As well as outputting the pressure at these points, which can be used to obtain the normal and tangential forces on the blade, the flow patterns around the blade and in the wake downstream are also modelled at the chosen mesh resolution.

The detail of the CFD approach comes at the expense of computational time, and often BEMT is favoured as a first approach to develop a blade design through investigation of the blade power capture and thrust loading. CFD is often used secondarily for detailed structural design, and to investigate specific issues such as cavitation [6], [7].

While BEMT was initially designed to model turbine loading in steady state conditions in a uniform current with depth, the method has been developed to take into account shear currents and dynamic loads from combined waves and currents ([8], [9]), although to the authors' knowledge turbulence has yet to be fully accounted for in this approach. CFD models can also be run with steady or dynamic inputs, although transient analyses considerably increase the computational time. [10] and [11] present CFD simulations with shear current, and [12], [13] with combined waves and current. A range of turbulence models have been used in these CFD models. [14] used the k-epsilon model, although [12] recommend the SST model for this application, in agreement with [15] who tested a range of turbulence models against experimental data in the context of wind turbines.

Several studies have compared the results from BEMT, CFD and experiments. A number of these have found that CFD models predict higher forces compared to BEMT ([16], [17]), although [18] showed that CFD could either under or over predict the forces compared to BEMT, depending on the tip speed ratio. It is, therefore, likely that the extent of the differences between the model predictions will depend on the details of each model formulation and the chosen simulation conditions.

[19] and [20] developed a combined modelling approach that uses the simplicity of BEMT to reduce the computational time of a 3D CFD model in order to study turbine wake characteristics. The 3D CFD model of the flow field is used to determine the inflow vector for input into the BEMT model and the thrust and torque outputs from BEMT are used to define momentum and swirl changes in the 3D CFD model, thereby avoiding the need for detailed CFD modelling in the region around the turbine blades.

In a similar way, the aim of this paper is to combine BEMT and CFD approaches to develop a more efficient methodology; in this case in order to obtain the pressure distribution over the blade surface. The proposed approach is expected to be particularly useful during the initial design stages where it is envisaged that structural analysis and optimisation studies will benefit from the greater level of detail provided by this method, particularly in structurally sensitive areas such as the thin trailing edge, without the need for long model run times.

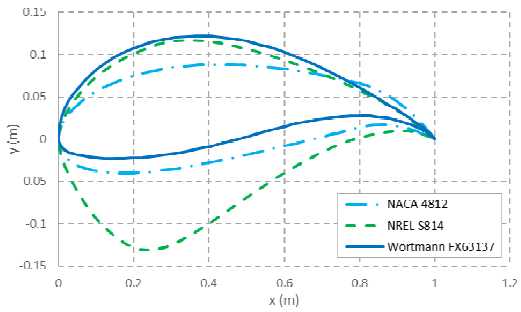

Fig. 1 Aerofoil sections chosen for models (before chord and twist has been applied).

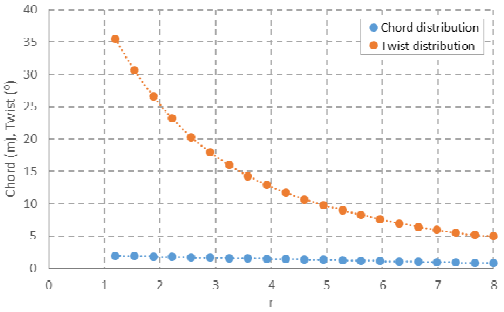

Fig. 2 Chord and twist distributions for modelled blades.

TABLE I
INPUT PARAMETERS FOR MODELS

Parameter	Value in full scale model	Value in small scale model
Flow velocity (m/s)	2.5	0.625
TSR	4	4
Water depth at hub centre (m)	35	2.1875
Number of blades	3	3
Turbine diameter (m)	16	1
Blade length (m)	6.8	0.425

The model developed uses the inflow velocity vector computed for each blade element in the BEMT model as inputs to a set of 2D CFD models of the sections along the blade radius. Combining the results from the set of 2D CFD models provides a detailed map of the pressure distribution over the blade but at a much reduced computational cost compared to 3D CFD modelling.

The new modelling approach is tested against BEMT and 3D CFD models to assess its performance. This is completed for three different blade profiles to check for any geometry dependence. The models are run at field scale in the first instance. The effect of Reynolds number on the model agreement is then considered by comparing the results of one of the blade geometries run at small scale (1 m turbine diameter), where the input parameters are Froude scaled from the larger model.

The paper begins by setting out the methodology for each model in Section II. The results from the new modelling approach are then presented in Section III before the comparison between these results with the BEMT and the 3D CFD models are discussed in Section III a and b. In Section

IV the models are then compared in terms of resolution, accuracy and computational time to assess the merits of the proposed method for solving tidal turbine blade design problems.

II. Methodology

To test the validity of the proposed 2D-CFD-BEMT method and to compare this with the BEMT and 3D CFD approaches, three different blade geometries were selected for comparison. These were chosen to provide a range of shapes in terms of the aerofoil thickness and have all been used in previous tidal turbine blade studies [21]-[23]. The three profiles are plotted (prior to the twist and chord distributions being applied) in Figure 1. To make the comparison consistent, the chord and twist distribution along the radius of the blade were set equal for each of the blade geometries; the distributions are shown in Figure 2. The aim of comparing the model results for three blade designs is to investigate if the model agreement is affected by the aerofoil geometry, namely due to changes in flow separation and the lift and drag coefficients.

To run the simulations, the input parameters were set as shown in Table I. The main comparison was conducted at full scale to demonstrate direct relevance to tidal turbine design. A second comparison at smaller scale was conducted for the NREL blade, and the input parameters are also given in Table 1. At this stage the comparison is conducted for typical rather than extreme operating environments and under steady state conditions.

A. BEMT model

Many texts provide a comprehensive description of blade element momentum theory (see for example [24]) so a detailed treatment of its derivation is not given here, rather an overview of the approach is offered.

BEMT combines two theories, momentum theory and blade element theory, in order to generate the number of equations required to solve for the number of unknowns. Momentum theory provides two equations, one for the thrust and one for the torque on the blade, but with two further unknowns, the axial and angular induction factors.

Blade element theory provides alternative equations for the torque and thrust, in relation to the axial and angular induction factors and lift and drag coefficients. Hence by combining these four equations, and providing inputs for the lift and drag coefficients (from experimental data or using a computational approach such as XFOIL) the four unknowns can be solved.

As these equations are implicit, they must be solved iteratively or by using an optimisation function, both of which can introduce error due to the potential for non-convergence of the solution.

The set of four equations is solved at a specified number of elements along the blade radius. The greater the number of elements used, the better the resolution of forces along the blade and the higher the accuracy of the total thrust and torque per blade.

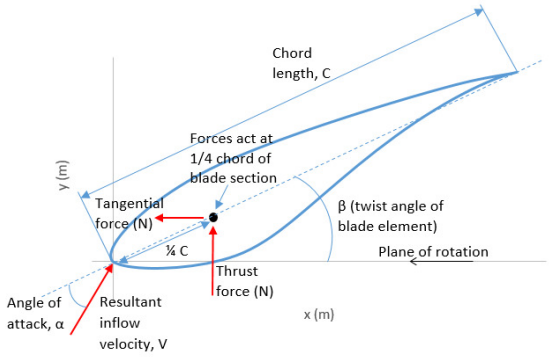

Fig. 3 Outputs from the BEMT model for one blade section.

The outputs of the BEMT model are illustrated in Figure 3. The thrust and torque are defined perpendicular and parallel to the plane of rotation, and the axial and angular induction factors determine the magnitude of the resultant inflow velocity and its direction (angle of attack) per element along the blade. The BEMT outputs apply to the midpoint of each element along the blade radius, with each element forming an annulus in the rotor plane. Thus to obtain the forces per blade the torque and thrust values must be divided by the number of blades on the turbine.

From Figure 3 it is clear that the BEMT model does not give the distribution of pressure over the blade but only the resolved force components for each blade element used in the computation. The model developed in this paper in Section II c presents a method to obtain a detailed pressure map from the BEMT outputs.

The main advantages of the BEMT approach are its simplicity and low computational cost. Its limitations are that it does not consider turbulence in the inflow current (although some turbulence effects may be included through the lift and drag coefficients), and it assumes there is no radial flow. Momentum theory also assumes an infinite number of turbine blades (porous disk). The accuracy of the solution depends on the strength of the iteration or optimisation procedure used and the convergence criteria or minimisation error set.

A number of modifications to the original BEMT have been proposed to account for some of these limitations in the model.

[25] discussed the Prandtl tip loss correction and developed this to include hub losses, to account for radial flow which is significant in these locations.

Correction factors have also been proposed by [26]-[28] to apply to cases with a high angle of attack, where the momentum theory is not valid (see [24]).

The results of the BEMT approach are heavily dependent on the method used to compute the lift and drag coefficients. Whether experimental or numerical data is used, whether this data was collected at the appropriate Reynolds number, and whether the lift and drag data were obtained from a two-dimensional or three-dimensional model all affect the outcome.

While 3D lift and drag coefficients (i.e. including rotational effects) are more representative of the tidal turbine application, these types of experiments are much more difficult to run and

consequently fewer data sets are available. Therefore, 2D data is often used.

[29] found that 2D lift and drag coefficients work well in the attached regime. They developed empirical equations to adjust the lift and drag coefficients in the stall regime to provide a post-stall correction to the 2D coefficients to improve the BEMT model performance under these conditions. The BEMT approach used in the present study [9] applies the Bhul, Prandtl and Viterna & Corrigan correction factors.

B. 3D CFD model

The 3D CFD modelling was conducted using Ansys Fluent.

Symmetry was applied so that the model need only consist of one blade and a segment shaped domain around it i.e. covering 1/3rd of a circle, see Figure 4. Periodic boundaries were applied to the cross-stream faces of the domain to take into account the influence of the other blades on the modelled one. The inlet boundary was positioned 15 m upstream of the blade with a radius of 35 m with the boundary condition set to the inflow velocity specified in Table I. The outlet boundary radius was 45 m, positioned 20 m downstream of the blade with the boundary condition set to the ambient static pressure. The domain had 2474580 elements with variable mesh density.

The rotational effects were modelled by using a rotating domain set at the turbine rotational speed corresponding to the parameters specified in Table I (1.125 rad/s).

The no slip shear condition, and standard k-epsilon turbulence model were applied. This steady state model converged within 1500 iterations, taking approximately 2.5 hours to run.

For the model comparison in this paper the 3D CFD model results of interest were the pressure output at each node of the mesh over the blade surface specified in (x, y, z) coordinates.

C. 2D-CFD-BEMT model

In the combined 2D-CFD-BEMT approach, the results from the BEMT model described previously in section II a (i.e. output angle of attack and magnitude of inflow velocity per blade element) are used to provide the flow input to the inlet boundary of a 2D-CFD model of each blade section. The 2D blade sections modelled in the 2D-CFD simulations are set at the mid-points of the elements used in the BEMT model.

The 2D-CFD model uses a D-shaped domain around a single blade section with a chord of 1 m. The domain has a total width of 25 m, see Figure 5.

A script was set-up to apply a scale factor to this blade section in a series of runs (in a loop) to replicate each section along the blade radius from the BEMT model in terms of the chord distribution. The code also provides the inflow velocity vector derived from the BEMT model for each section. Note the scale factor is applied to the mesh as well as the blade geometry.

The same settings were used in the 2D CFD simulations as in the 3D simulations (i.e. k-epsilon turbulence model, no slip condition). Periodic boundaries were set in the cross-stream directions as this allows the angle of inflow to be varied without having to change the computational domain. Ambient static pressure was applied at the outlet boundary.

The pressure at each mesh node (x, y coordinates) around the blade section output from the 2D CFD section runs were split into those corresponding to the upper and lower blade halves and linked with the z coordinate (radial position along the blade known from the BEMT model). The twist angle (specified in Figure 2) is then applied to the x and y coordinates of the 2D CFD data for each section to reconstruct the original blade geometry. MATLAB was used to combine the pressure data from each section in one plot of the blade and a linear interpolation function was applied to obtain the pressure distribution in-between each blade section. This worked best by interpolating the data separately for the upper and lower blade halves, to enable the interpolation to proceed smoothly along the blade surface.

The full set of 2D CFD sections takes only a few minutes to run. Processing and plotting the data and applying the interpolation function using a script in MATLAB adds only a few minutes onto the approach.

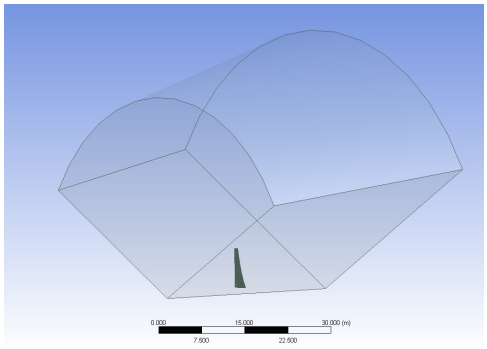

Fig. 4 CFD domain for steady state 3D model with symmetry.

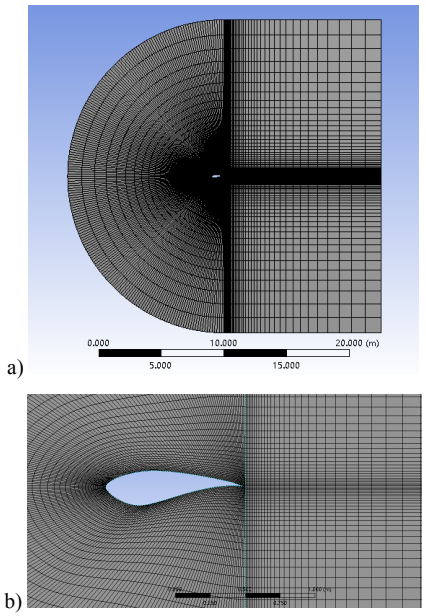

Fig. 5 CFD domain for steady state 2D model a) full domain b) close up of mesh around the aerofoil.

a)

b)

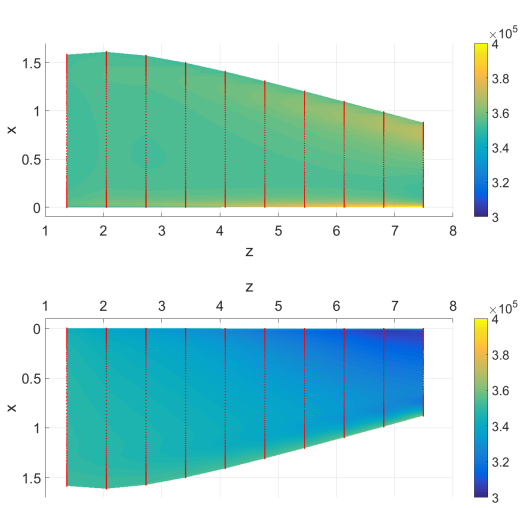

Fig. 6 2D-CFD-BEMT model results for NACA a) lower blade surface b) upper blade surface.

a)

b)

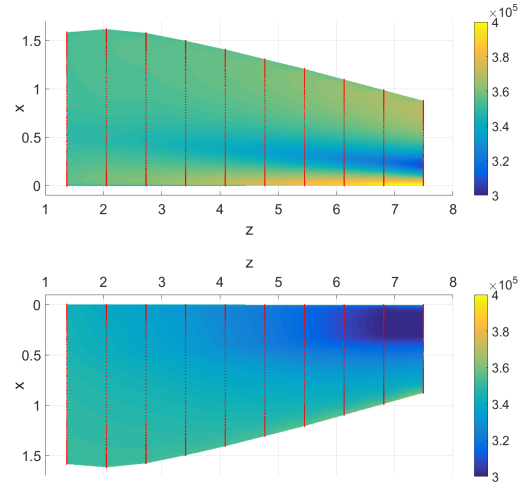

Fig. 7 2D-CFD-BEMT model results for NREL a) lower blade surface b) upper blade surface.

a)

b)

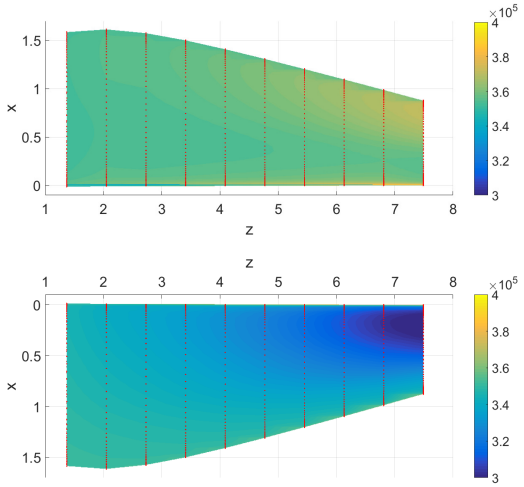

Fig. 8 2D-CFD-BEMT model results for Wortmann a) lower blade surface b) upper blade surface.

Note that in this paper the BEMT model was run with 20 elements, as this was found to produce stable results. 10 sections were run in the 2D-CFD-BEMT model located at the centre of every other element used in the BEMT model. This enabled comparisons to be made and the interpolation function to be tested, but obviously using more sections along the blade will improve the resolution of the model. Having used 10 sections in this study to provide a demonstration of the approach, it would be appropriate to use more sections in future when applying this model to real design problems.

The 2D CFD models can also output the force components in the x and y directions. This allows direct comparison with the BEMT outputs of thrust and tangential force, once the 2D CFD forces have been realigned to take into account the twist of the blade sections (which is not needed in the 2D CFD models) and by multiplying the 2D CFD model forces by the width of the blade element used in the BEMT model.

III. Results

The resulting pressure distributions obtained from the combined 2D-CFD-BEMT modelling approach over the surface of each of the three selected blade profiles are shown in Figures 6-8. In each plot the sections that were used in the 2D CFD model are shown by the red dots marking the locations of the output pressure information. The MATLAB interpolation function shows the pressure distribution between these sections, and can be used to provide an estimate of the pressure value at any coordinate specified on the blade surface.

Note that the blade root and tip sections are not shown in the graphs as extrapolation was not used in this model. However, this could be added to estimate the pressure at the blade root and tip sections.

The high mesh resolution in the 2D CFD models results in good coverage along each blade section. The resolution along the blade radius can be improved by running a greater number of sections in the BEMT and 2D CFD codes, without substantially extending the computational time. However, the linear interpolation function has resulted in a smooth pressure distribution across the blade surfaces, and at this resolution may prove appropriate for initial analysis work.

The pressure distributions over the three blades are fairly similar, with the highest pressure occurring at the leading edge and increasing towards the blade tip, and the lowest pressure occurring on the upper side, decreasing towards the blade tip, as is to be expected (see for example [30] for qualitatively similar results of pressure distributions over turbine blades).

When comparing the results for the three blade geometries, the distance between the region of lowest pressure on the upper side and the leading edge varies a little between the three blade shapes, but the greatest variation is in the pressure distributions on the lower side of the blade. Here the region of low pressure over the thickest part of the blade varies most noticeably, with the NREL blade resulting in much lower pressure in this region near the blade tip than for the other two blades. This is a result of the much thicker, curvier section shape for the NREL compared to the NACA and Wortmann

profiles (see Figure 1) that changes the flow patterns and point of separation around the aerofoil.

While qualitatively the 2D-CFD-BEMT model results are satisfactory, to better understand the performance of the 2D-CFD-BEMT approach, it is compared firstly with BEMT model results and then with a 3D CFD model in the following two sections.

A. Comparison of BEMT and 2D-CFD-BEMT model results

The normal and tangential forces output from the BEMT model and also output from the 2D-CFD-BEMT simulations for each section along the blade radius are compared for the three blade aerofoil profiles in Figure 9. Note that only the dynamic force is compared i.e. the hydrostatic force is not included. The shape of the curves is in good agreement between the models. However, the BEMT approach results in both higher normal and tangential forces than from the combined 2D-CFD-BEMT model.

a)

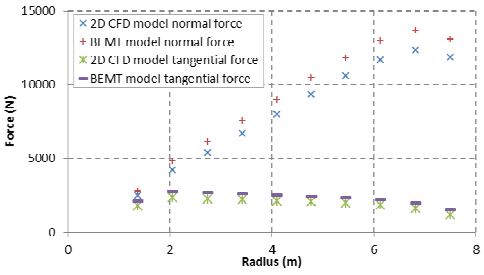

b)

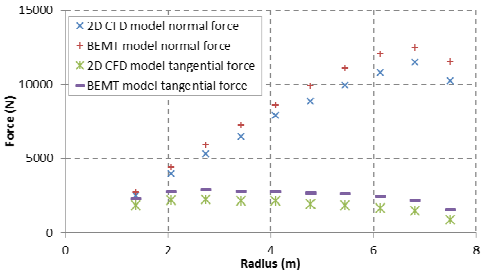

c)

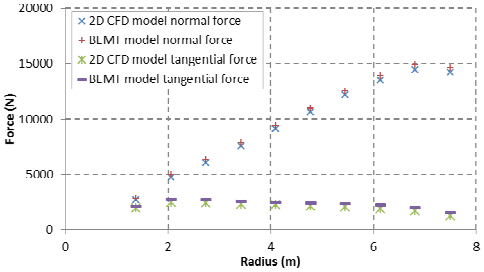

Fig. 9 Comparison of BEMT and 2D-CFD-BEMT model results for normal and tangential force components along a) NACA blade, b) NREL blade, c) Wortmann blade.

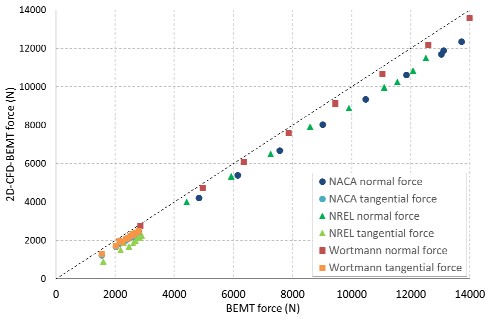

Fig. 10 Normal and tangential force components computed from the BEMT and 2D-CFD-BEMT models for the three blade geometries.

TABLE II
COMPARISON OF MODEL AGREEMENT FOR THE THREE BLADE PROFILES

	Normal force		Tangential force	
Blade profile	**Maximum difference (%)**	**Average difference (%)**	**Maximum difference (%)**	**Average difference (%)**
NACA	13.5	11.6	22.6	17.4
NREL	11.9	10.2	56.2	32.0
Wortmann	4.5	3.5	19.7	13.2

To understand the extent of agreement between the models, the percentage difference between the forces is calculated. The average and maximum percentage difference for each case is presented in Table II. The agreement is significantly poorer for the tangential forces compared to the normal forces in each case when considering the difference as a percentage of the mean values. As the tangential forces are much smaller than the normal forces, it is anticipated that inaccuracies in the tangential forces would only have a small effect on the results of a structural analysis.

B. Comparison of 3D CFD and 2D-CFD-BEMT model results

To compare the 2D-CFD-BEMT model with the 3D CFD model, the coordinates of the pressure points output from the 3D CFD model are matched in the 2D-CFD-BEMT model by using the interpolation function to estimate the pressure values at these coordinates. This provides a set of commonly located points in both approaches. In Figure 11 the pressure at each of these points is directly compared by plotting one against the other. Points sitting on the identity line in the graphs indicate perfect agreement between the models. Qualitatively the agreement is reasonable in Figure 11 although there are a number of points where the agreement is noticeably poorer. It is clear in Figure 11 that the 2D-CFD-BEMT model both under and over predicts the pressure compared to the 3D CFD model.

To investigate any patterns in the over/under prediction of the 2D-CFD-BEMT results compared to the 3D CFD results and determine the locations on the blade with the best and worst model agreement, Figures 12-14 plot the percentage increase/decrease in pressure across the blade surface, where a positive value indicates that the pressure is higher in the 2D-CFD-BEMT model than that in the 3D CFD model. The red dots plotted indicate the common points in the two models

that have been compared. A linear interpolation function is used to show the distribution of the percentage difference in pressure between the two models.

Figures 12-14 show that the agreement between the two models over much of the blade surface is very close. However, the model agreement consistently reduces towards the blade tip area, and particularly along the leading edge for each of the blade geometries.

Unique to the lower surface of the NREL blade is poorer agreement in the tip area at the thickest part of the aerofoil. This is probably due to complexities in the flow caused by the thicker aerofoil compared to the NACA and Wortmann profiles.

a)

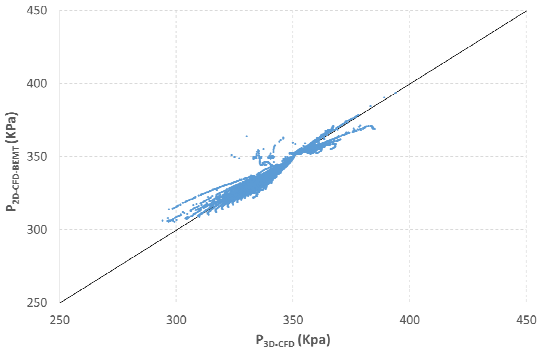

b)

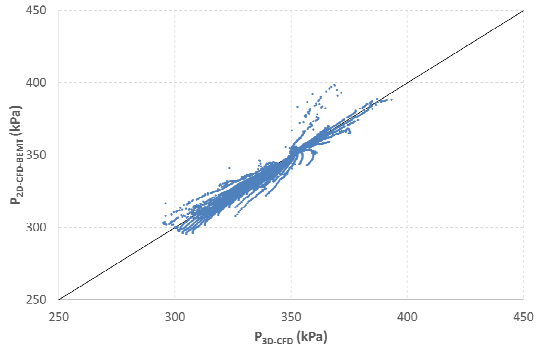

c)

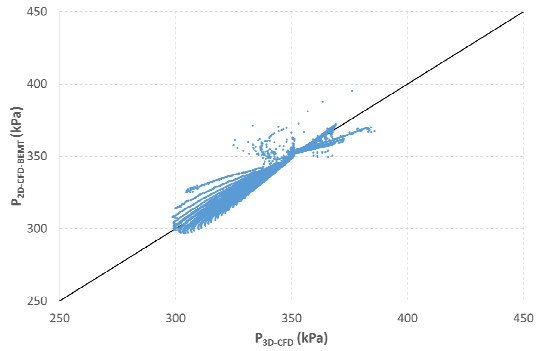

Fig. 11 Comparison of 3D CFD and 2D-CFD-BEMT model results of the pressure at the same points on the a) NACA b) NREL c) Wortmann blade surface.

a)

b)

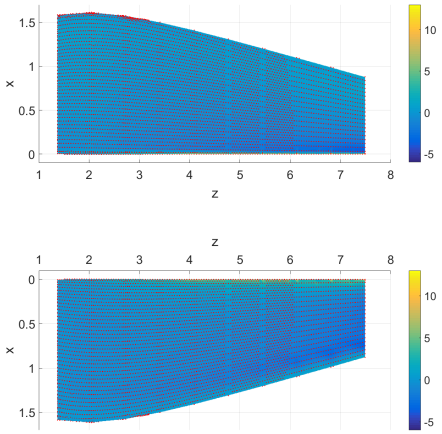

Fig. 12 Comparison of the percentage difference in pressure between the 3D CFD and 2D-CFD-BEMT model results, with positive values indicating higher pressure in the 2D-CFD-BEMT model than in the 3D CFD model, for NACA a) lower blade surface b) upper blade surface.

a)

b)

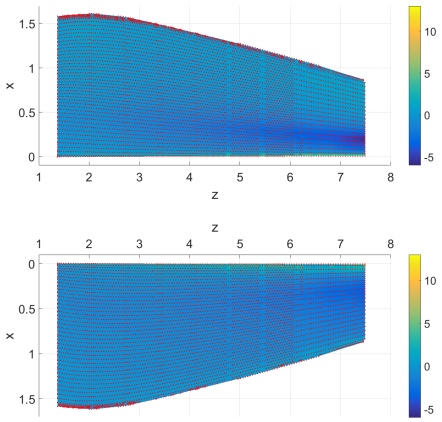

Fig. 13 Comparison of percentage difference in pressure between 3D CFD and 2D-CFD-BEMT results, with positive values indicating higher pressure in the 2D-CFD-BEMT model than in the 3D CFD model, for NREL a) lower blade surface b) upper blade surface.

a)

b)

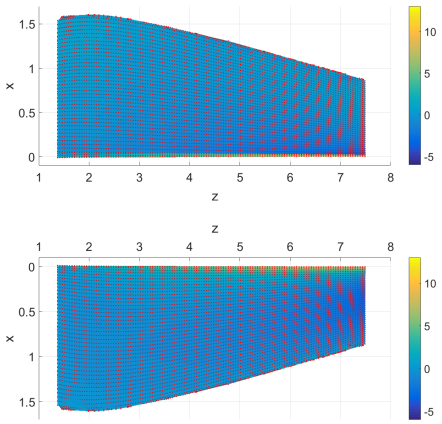

Fig. 14 Comparison of percentage difference in pressure between 3D CFD and 2D-CFD-BEMT results, with positive values indicating higher pressure in the 2D-CFD-BEMT model than in the 3D CFD model, for Wortmann a) lower blade surface b) upper blade surface.

TABLE III
COMPARISON OF MODEL AGREEMENT FOR THE THREE BLADE PROFILES

Blade profile	Percentage of points with <5% difference between models (%)	Maximum difference between points (%)
NACA	99.8	9.8
NREL	99.6	8.7
Wortmann	98.9	10.8

C. *Effect of Reynolds number on the results*

To gain further confidence in the 2D-CFD-BEMT modelling approach, a second comparison was made between the models under different ambient conditions, representative of small scale laboratory testing. The turbine diameter was set to 1 m and the input parameters were Froude scaled accordingly (see Table 1), so that this resulted in the Reynolds number being reduced from $8.11e^6$ to $1.27e^5$. It is well known that the Reynolds number has a significant influence on the flow patterns around aerofoils [31] and it is important to understand the model performance at small scale to enable comparison with experimental data.

The 2D-CFD-BEMT results for the NREL blade are shown in Figure 15. The pressure distribution is qualitatively very similar to that at the full scale shown in Figure 7.

In Figure 16 the 2D-CFD-BEMT results are compared with the BEMT normal and tangential forces along the blade radius. Two runs of the BEMT model are included in the comparison, one using lift and drag coefficients computed from XFOIL ($Re=4.4e^5$) following the same methodology as used in the previous full scale comparison, and a second run where the lift and drag coefficients were obtained from the experimental data of [32] for the NREL aerofoil at a similar Reynolds number ($5.1e^4$) to that of the scaled model. It is seen in Figure 16 that the agreement between the models with the XFOIL data is poorer than at the larger scale, but by using the experimental data in the BEMT model the agreement is improved considerably. This is in agreement with previously reported limitations of the XFOIL model at lower Reynolds numbers, where XFOIL has been found to tend to over-predict the lift and drag coefficients [33]. As with the larger scale simulations, the agreement is better for the normal forces than for the tangential forces. The agreement is quantified in Table IV. While the agreement for the normal force using the experimental lift and drag coefficients is as good as that at the full scale, the agreement in the tangential forces is much poorer at this small scale.

In Figures 17 and 18 the 2D-CFD-BEMT model results are compared with the 3D CFD results. Similarly to the larger scale simulations the 2D-CFD-BEMT model both under and over predicts the pressure compared to the 3D CFD model data and the agreement is poorest on the upper blade surface near the leading edge towards the blade tip. For this comparison 98.3% of the points compared had a percentage difference less than 5%, and the maximum percentage difference was 12.1%, which shows that the agreement between the models has reduced a little compared to that at the full scale.

a)

b)

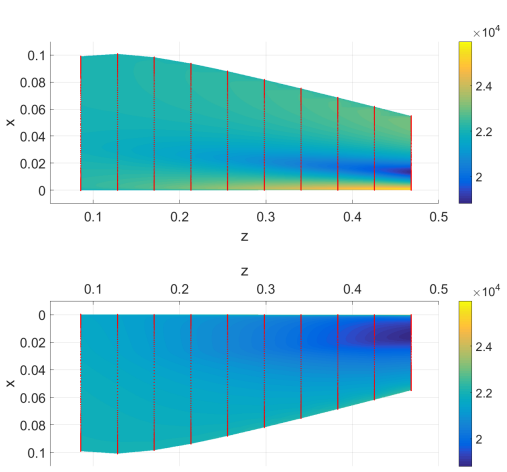

Fig. 15 2D-CFD-BEMT model results for NREL S814 1m diameter turbine a) lower blade surface b) upper blade surface.

a)

b)

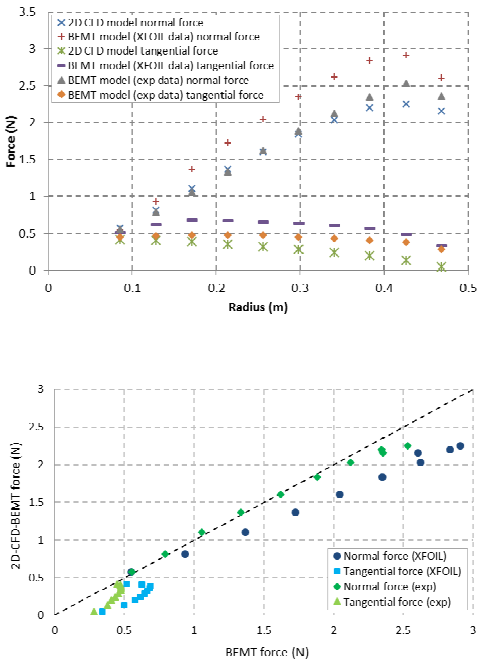

Fig. 16 Comparison of BEMT and 2D-CFD-BEMT model results for NREL blade (1m diameter turbine), a) normal and tangential force components along the blade radius, b) BEMT normal and tangential forces plotted against 2D-CFD-BEMT normal and tangential forces.

TABLE IV
COMPARISON OF MODEL AGREEMENT BETWEEN 2D-CFD-BEMT AND BEMT APPROACHES, WITH DIFFERENT LIFT AND DRAG INPUTS TO THE BEMT MODEL.

	Normal force		Tangential force	
Lift and drag inputs	**Maximum difference (%)**	**Average difference (%)**	**Maximum difference (%)**	**Average difference (%)**
XFOIL	25.5	20.6	152.6	78.3
Experiment	11.6	4.9	144.0	52.3

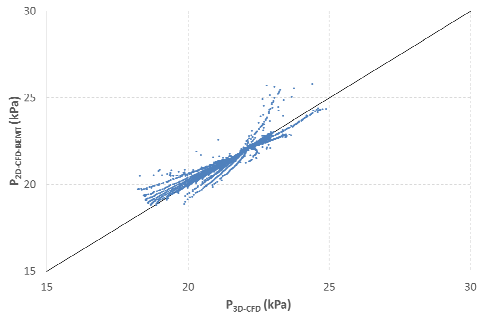

Fig. 17 Comparison of 3D CFD and 2D-CFD-BEMT results for pressure at the same points on the NREL blade surface (1m diameter turbine).

a)

b)

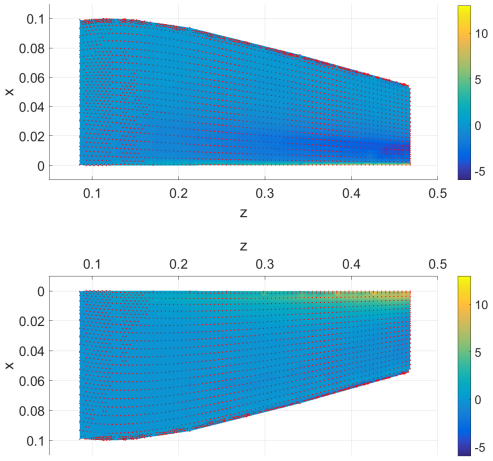

Fig. 18 Comparison of percentage difference in pressure between 3D CFD and 2D-CFD-BEMT results, with positive values indicating higher pressure in the 2D-CFD-BEMT model than in the 3D CFD model, for NREL (1m diameter turbine) a) lower blade surface b) upper blade surface.

IV. Discussion

The comparisons in the previous sections have shown that the 2D-CFD-BEMT approach agrees reasonably well with both the BEMT and 3D CFD results. Compared to BEMT, the model consistently under-predicts the normal and tangential forces. This is probably attributable to limitations in the computation of the lift and drag coefficients in XFOIL compared to in the CFD model.

Compared to the 3D-CFD model results, the 2D-CFD-BEMT model consistently resulted in a more extreme pressure distribution so that areas of higher pressure were higher, and areas of lower pressure were lower than in the 3D CFD model. These differences may be because the 2D-CFD-BEMT model does not fully account for rotational effects. The angle of attack is determined in BEMT based on the turbine rotational speed, but in the 2D-CFD models the flow itself develops around the aerofoil sections in a stationary setting. Radial flow will also not be modelled as each blade section is considered independently which is not the case in the 3D CFD model.

The key advantage of the proposed approach is its fast computational time compared to 3D CFD modelling. For steady state solutions, it takes no more than 30 minutes to run the BEMT model, the 2D-CFD simulations and the MATLAB data processing routine, whereas the 3D CFD model takes approximately 2.5 hours.

While this is undoubtedly an efficiency saving, the modelling approach is not orders of magnitude quicker for steady state solutions and the additional detail and accuracy of the 3D CFD model may make it worthwhile to run 3D CFD simulations for these cases.

Where the proposed approach is anticipated to provide worthwhile efficiency savings is when running dynamic models. Here the BEMT model time increases to an hour or so (depending on the length of the time series to be modelled) but the 3D CFD model time increases to the order of days or weeks even for short time series.

For dynamic loading, one approach would be to run the BEMT model to provide an overview of the loading patterns through time. Points of interest such as when the maximum loads occur on the blades could then be picked out and run through the 2D-CFD-BEMT approach to investigate the pressure distribution using the proposed method. This would save a significant amount of time compared to conducting 3D CFD modelling. It would also be possible to run the 2D-CFD-BEMT model for every time step of the BEMT simulation. This would increase the time for the modelling, but it would still be orders of magnitude quicker than a 3D CFD model for the same length of simulation time. It would also enable longer simulation times to be investigated than is really feasible with 3D-CFD models.

In this way the model could be very useful for preliminary structural design and analysis, particularly when considering the fatigue life of the blade, as well as investigating the details of failure modes such as delamination which often occur along the blade trailing edge.

V. Conclusion

This paper presents a method for obtaining the pressure distribution over a tidal turbine blade by using a combined 2D-CFD-BEMT approach where the outputs from the BEMT model in the form of the magnitude and angle of attack of the resultant inflow velocity per blade element are input to a set of 2D CFD models for each of the blade sections along the blade radius. This enables the 2D pressure distribution around the sections to be modelled, and using an interpolation function the 3D pressure distribution between the sections over the full blade can be estimated.

It was determined that this method provides reasonable agreement with both BEMT and 3D CFD models for a range of blade profiles and at different Reynolds numbers. BEMT consistently over-predicts the forces compared to the combined 2D-CFD-BEMT approach, which may be due to the use of XFOIL to compute the lift and drag coefficients in the BEMT model, while the 3D-CFD model results in pressure distributions with a smaller difference between areas of high and low pressure, which is probably a result of more accurately modelling the effects of turbine rotation on the flow patterns around the blade. The model agreement was better at larger scale (higher Reynolds number), which can be

explained by known limitations in XFOIL in the lower Reynolds number range.

The modelling approach successfully reduces the computational time required compared to 3D CFD modelling. This is especially true when considering dynamic loading, where the run times for 3D CFD models are orders of magnitude larger.

With the combined 2D-CFD-BEMT approach points of interest in a time series run in a dynamic BEMT model can be selected and the pressure distribution over the blade surface obtained. The pressure distribution can also be output for all time steps in the model in considerably quicker time than using a 3D CFD model.

The 2D-CFD-BEMT model is, therefore, useful during the first stage of design and optimisation in terms of assessing the structural and fatigue performance of tidal turbine blades, and it provides an efficient approach to try many design iterations that are based on detailed load distributions over the blade surface.

ACKNOWLEDGMENT

This research was funded by the EPSRC.

REFERENCES

[1] MeyGen (2013) Phase 1a. [Online]. Available: www.meygen.com

[2] P. Liu and B. Veatch, "Design and optimization for strength and integrity of tidal turbine rotor blades," *Energy*, vol. 46(1), pp. 393-404, 2012.

[3] N. Barltrop, K. S. Varyani, A. Grant, D. Clelland and X. P. Pham, "Investigation into wave-current interactions in marine current turbines," *Proceedings of the Institution of Mechanical Engineers Part A: Journal of Power and Energy*, vol. 221, pp. 233-242, 2007.

[4] P. W. Galloway, L. E. Myers and A. S. Bahaj, "Quantifying wave and yaw effects on a scale tidal stream turbine," *Renewable Energy*, vol. 63, pp. 297-307, 2014.

[5] SI Ocean (2012) Ocean energy: state of the art. [Online]. Available: http://www.si-ocean.eu/en/Technology-Assessment/Overview/

[6] B.-S. Kim, M.-E. Kim, and W.-J. Kim, "A study on the design and performance prediction of MW class ocean current turbine," *3rd International Conference on Ocean Energy*, Bilbao, Spain, 2010.

[7] P. M. Singh, and Y.-D. Choi, "Shape design and numerical analysis on a 1 MW tidal current turbine for the south-western coast of Korea," *Renewable Energy*, vol. 68, pp. 485-493, 2014.

[8] C. Faudot, and O.G. Dahlhaug, "Prediction of wave loads on tidal turbine blades," *Energy Procedia*, vol. 20, pp. 116-133, 2012.

[9] T. M. Nevalainen, C. M. Johnstone and A. D. Grant, "An unsteady blade element momentum theory for tidal stream turbines with morris method sensitivity analysis," *Proceedings of the 11th European Wave and Tidal Energy Conference*, Nantes, France, 2015.

[10] A. Mason-Jones, D. M. O'Doherty, C. E. Morris and T. O'Doherty, "Influence of a velocity profile and support structure on tidal stream turbine performance," *Renewable Energy*, vol. 52, pp. 23-30, 2013.

[11] J. McNaughton, S. Rolfo, D. D. Apsley, T. Stallard amd P. K. Stansby, "CFD power and load prediction on a 1MW tidal stream turbine with typical velocity profiled from the EMEC test site," *10th European Wave and Tidal Energy Conference*, Aalborg, Denmark, 2013.

[12] S. C. Tatum, C. H. Frost, M. Allmark, D. M. O'Doherty, A. Mason-Jones, P. W. Prickett, R. I. Gosvenor, C. B. Byrne and T. O'Doherty, "Wave-current interaction effects on tidal stream turbine performance and loading characteristics," *International Journal of Marine Energy*, vol. 14, pp. 161-179, 2016.

[13] M. A. Holst, O. G. Dahlhaug and C. Faudot, "CFD analysis of wave-induced loads on tidal turbine blades," *IEEE Journal of Oceanic Engineering*, vol. 40(3), pp. 506-521, 2015.

[14] I. Masters, A. Williams, T. N. Croft, M. Togneri, M. Edmunds, E. Zangiabadi, I. Fairley and H. Karunarathna, "A comparison of numerical modelling techniques for tidal stream turbine analysis," *Energies*, vol. 8(8), pp. 7833-7853, 2015.

[15] W. T. Kirk, V. R. Capece, G. Pechlivanoglou, C. N. Nayeri and C. O. Paschereit, "Comparative study of CFD solver models for modeling of flow over wind turbine airfoils," *ASME Turbo Expo 2014: Turbine Technical Conference and Exposition*, Dusseldorf, Germany.

[16] M. J. Lawson, Y. Li and D. C. Sale, "Development and verification of a computational fluid dynamics model of a horizontal-axis tidal current turbine," *ASME 30th International Conference on Ocean, Offshore, and Arctic Engineering*, Rotterdam, The Netherlands, 2011.

[17] P. B. Johnson, G. I. Gretton and T. McCombes, "Numerical modelling of cross-flow turbines: a direct comparison of four prediction techniques," *3rd International Conference on Ocean Energy*, Bilbao, Spain, 2010.

[18] J. H. Lee, S. Park, D. H. Kim, S. H. Rhee and M.-C. Kim, "Computational methods for performance analysis of horizontal axis tidal stream turbines," *Applied Energy*, vol. 98, pp. 512-523, 2012.

[19] S. R. Turnock, A. B. Phillips, P. J. Banks and R. Nicholls-Lee, "Modelling tidal current turbine wakes using a coupled RANS-BEMT approach as a tool for analysing power capture of arrays of turbines," *Ocean Engineering*, vol. 38, pp. 1300-1307, 2011.

[20] R. Malki, A. J. Williams, T. N. Croft, M. Togneri and I. Masters, "A coupled blade element momentum – computational fluid dynamics model for evaluating tidal stream turbine performance," *Applied Mathematical Modelling*, vol. 37, pp. 3006-3020, 2013.

[21] T. P. Lloyd, S. R. Turnock and V. F. Humphrey, "Unsteady CFD of a marine current turbine using Open Foam with generalized grid interface," *Proceedings of the 14th Numerical Towing Tank Symposium*, Poole, UK, 2011.

[22] D. A. Doman, R. E. Murray, M. J. Pegg, K. Gracie, C. M. Johnstone, and T. Nevalainen, "Tow-tank testing of a 1/20th scale horizontal axis tidal turbine with uncertainty analysis," *International Journal of Marine Energy*, vol. 11, pp. 105-119, 2015.

[23] C. Frost, C. E. Morris, A. Mason-Jones, D. M. O'Doherty and T. O'Doherty, "The effect of tidal flow directionality on tidal turbine performance characteristics," *Renewable Energy*, vol. 78, pp. 609-620, 2015.

[24] M. O. L. Hansen, *Aerodynamics of wind turbines*, London, UK: Earthscan, 2008.

[25] P. J. Moriarty and A. C. Hansen, "AeroDyn theory manual," National Renewable Energy Laboratory, Tech. Rep. NREL/TP-500-36881, 2005.

[26] M. L. Bhul, "A new empirical relationship between thrust coefficient and induction factor for the turbulent windmill state," National Renewable Energy Laboratory, Tech. Rep. NREL/TP-500-36834, 2005.

[27] D. A. Spera, *Wind turbine technology fundamental concepts of wind turbine engineering*, New York, USA: ASME Press, 1994.

[28] H. Glauert, "Airplane propellers," in *Aerodynamic Theory*, W. F. Durand, Ed., pp. 169-360. Springer, Berlin, Heidelberg, 1935.

[29] L. A. Viterna and R. D. Corrigan, "Fixed pitch rotor performance of large horizontal axis wind turbines," *DOE/NASA Workshop on Large Horizontal Axis Wind Turbines*, Cleveland, OH, USA. 1981.

[30] G. S. Bir, M. J. Lawson and Y. Li, "Structural design of a horizontal-axis tidal current turbine composite blade," *ASME 30th International Conference on Ocean, Offshore, and Arctic Engineering*, Rotterdam, The Netherlands, 2011.

[31] E. N. Jacobs and A. Sherman, "Airfoil section characteristics as affected by variations of the Reynolds number," National Advisory Committee for Aeronautics, Tech. Rep. 586, 1937.

[32] M. Togneri, I. Masters, R. Malki and A. Rio, "Flume measurements of lift and drag for selected tidal turbine blade sections," [Unpublished paper] College of Engineering, Swansea University, 2014.

[33] M. Drela, "Xfoil: an analysis and design system for low Reynolds number airfoils," *Low Reynolds Number Aerodynamics, Lec. Notes in Eng.*, vol. 54, pp. 1-12, 1989.